# *Ab initio* analytical model of light transmission through a cylindrical subwavelength hole in an optically thick film

V. G. Bordo*

*NanoSyd, Mads Clausen Institute, Syddansk Universitet, Alsion 2, DK-6400 Sønderborg, Denmark*

(Received 25 January 2011; revised manuscript received 21 July 2011; published 12 August 2011)

The rigorous analytical theory of light transmission through a cylindrical hole of arbitrary diameter in an optically thick film is developed. The approach is based on the introduction of fictitious surface currents at both hole openings and both film surfaces. The solution of Maxwell's equations obeying the boundary conditions at all interfaces is obtained in the form of the Fourier integral over the axial-wave-vector component. The exact integral equation which determines the field-amplitude Fourier transforms is derived. The general approach is simplified in the case of an elongated hole, where the film thickness considerably exceeds the hole diameter. It is emphasized that a specific pole corresponding to excitation of surface plasmon polaritons does not appear in the analysis. The theory is illustrated by the calculation of light transmission through a subwavelength hole in an Ag film.

DOI: 10.1103/PhysRevB.84.075465 PACS number(s): 78.67.−n, 42.25.Fx, 42.79.Ag

## I. INTRODUCTION

Since its discovery, the effect of the extraordinary optical transmission (EOT) has attracted considerable attention from both experimental and theoretical points of view.[1] Being first demonstrated for thin metal films perforated with subwavelength hole arrays,[2] this effect has been also studied in transmission through individual apertures in a metal screen.[3,4] The term "extraordinary" originates from the fact that at certain wavelengths the transmission efficiency normalized to the total area of the holes exceeds unity, which suggests that the metal film plays an active role in light transmission. This conclusion has led to the assumption that the EOT phenomenon is mediated by excitation of surface plasmon polaritons (SPPs). Extensive numerical calculations have been carried out aiming at explanation of this effect. Some of them claimed that EOT correlates with the excitation of SPPs in the metal film.[5–8] However, the other works which modeled the metal film by a perfect conductor (PC), which does not support SPPs, have also revealed enhanced light transmission.[9–12] Moreover, it was noticed that the SPP model is not consistent with all experimental observations.[13]

The reason for such contradictory explanations of EOT is the lack of a rigorous analytical theory and the use of various approximations whose validity is not well established. To interpret the EOT phenomenon, one needs to elucidate the light transmission through a single aperture. The first theoretical model developed for light diffraction at a subwavelength hole in an infinitely thin PC film was suggested by Bethe[14] and corrected for the near-field region by Bouwkamp.[15,16] Much later Roberts[17] calculated light transmission through a hole in a PC film of finite thickness using the so-called coupled-mode method. Although in its general formulation this method is rigorous, one should notice, however, that being cut at a certain maximum mode number it is not capable of describing accurately sharp edges of the hole.[5] The transmission properties of isolated apertures in real metals have been also studied theoretically using different numerical techniques such as the multiple multipole (MMP) technique,[5] the discrete sources method[8] (which is close to the MMP technique), the field-susceptibility technique (also known as Green's dyadic),[18,19] and the finite-difference time domain method.[6,7] Although these approaches provide rigorous solution of the problem, they require much computation time for convergence or have limited applicability. In addition, to discuss the physical background behind such calculations one needs to invoke simplified analytical models, which can result in misleading interpretation.

Recently, we have developed an analytical approach which allows one to obtain a rigorous solution of Maxwell's equations for a cylindrical resonator of finite length and of arbitrary radius.[20] This method is based on the introduction of fictitious electric and magnetic current sheets. A similar approach is applied here to the problem of light transmission through a cylindrical hole in an optically thick real metal film. The paper is organized as follows. In Sec. II we describe a general formalism and introduce the Hertz vectors and fictitious currents. We derive also an integral equation which determines the optical response of the system. In Sec. III we obtain an expression for the transmitted field and analyze it in the far-field limit. In Sec. IV the developed theory is applied to the case of an elongated hole. Section V illustrates this approach by the numerical calculations for an Ag film. In Sec. VI we discuss the role of SPPs in light transmission through a hole. Section VII summarizes the main results of the work.

## II. GENERAL THEORY

Let an infinite film of thickness $L$ have a circular cylindrical hole of radius $a$ with its axis perpendicular to the film surface [see Fig. 1(a)]. Let the film be characterized by the dielectric function $\epsilon_1(\omega)$, the hole be filled with the material having the dielectric function $\epsilon_2(\omega)$, and the film be surrounded by medium with the dielectric function $\epsilon_0$. We choose the origin of the cylindrical coordinate system $\mathbf{R} = (r,\theta,z)$ at the center of the hole and direct its $z$ axis along the hole axis from the entrance toward the exit hole opening.

 ©2011 American Physical Society

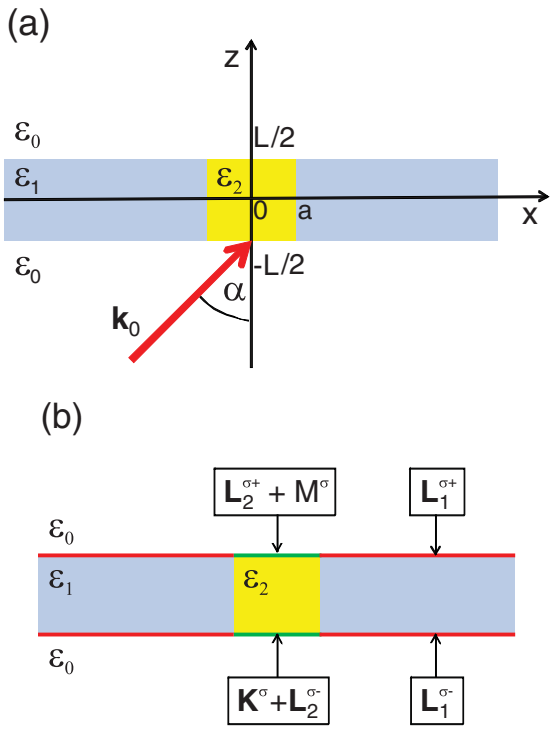


FIG. 1. (Color online) (a) Geometry of the problem. (b) The fictitious surface currents. The currents within the hole openings and out of them are indicated separately. The notations of the currents are explained in the text.

### A. Incident wave

Let us assume that a plane wave of frequency $\omega$ strikes the film surface under the angle $\alpha$ with respect to the $z$ axis so that its wave vector $\mathbf{k}_0$ lies in the $xz$ plane. Then its electric and magnetic field vectors can be written as

$$\mathbf{E}^i = \left(E^i_x \mathbf{e}_x + E^i_y \mathbf{e}_y + E^i_z \mathbf{e}_z\right) e^{i(k_{0x}x + k_{0z}z)} e^{-i\omega t} \tag{1}$$

and

$$\mathbf{H}^i = \left(H^i_x \mathbf{e}_x + H^i_y \mathbf{e}_y + H^i_z \mathbf{e}_z\right) e^{i(k_{0x}x + k_{0z}z)} e^{-i\omega t}, \tag{2}$$

respectively, where $\mathbf{e}_\mu$ are the unit vectors of the rectangular coordinates, $k_0 = (\omega/c)\sqrt{\epsilon_0}$, $c$ is the speed of light in vacuum, $k_{0x} = k_0 \sin\alpha$, and $k_{0z} = k_0 \cos\alpha$. The field components, $E^i_\mu$ and $H^i_\mu$, depend on the wave polarization. For the electric field vector parallel to the $xz$ plane ($p$ polarization),

$$\mathbf{E}^i = (-E_0 \cos\alpha, 0, E_0 \sin\alpha), \quad \mathbf{H}^i = (0, -H_0, 0), \tag{3}$$

whereas for the electric field vector parallel to the $y$ axis ($s$ polarization),

$$\mathbf{E}^i = (0, E_0, 0), \quad \mathbf{H}^i = (-H_0 \cos\alpha, 0, H_0 \sin\alpha). \tag{4}$$

Here $E_0$ and $H_0 = \sqrt{\epsilon_0} E_0$ are the electric and magnetic field amplitudes of the incident wave, respectively.

### B. Fictitious currents

A general solution of Maxwell's equations can be found in terms of the electric and magnetic Hertz vectors, $\mathbf{\Pi}^e$ and $\mathbf{\Pi}^m$, respectively.[21] Assuming the temporal dependence of the fields in the form of $\exp(-i\omega t)$, one can obtain the electric and magnetic field amplitudes in Gaussian units as follows:

$$\mathbf{E}_j = \nabla\left(\nabla \cdot \mathbf{\Pi}^e_j\right) + k_j^2 \mathbf{\Pi}^e_j + i\frac{\omega}{c} \nabla \times \mathbf{\Pi}^m_j, \tag{5}$$

$$\mathbf{H}_j = \nabla\left(\nabla \cdot \mathbf{\Pi}^m_j\right) + k_j^2 \mathbf{\Pi}^m_j - i\epsilon_j \frac{\omega}{c} \nabla \times \mathbf{\Pi}^e_j, \tag{6}$$

where $k_j = (\omega/c)\sqrt{\epsilon_j} = (2\pi/\lambda)\sqrt{\epsilon_j}$ with $\lambda$ the wavelength in vacuum and the subscript $j$ labels different media.

To construct the solution of Maxwell's equations in the film interior ($-L/2 < z < L/2$), we first find the fields which would be there in the absence of the hole. Such a solution can be found using standard methods.[22] The corresponding field components, $E_{1\mu}$ and $H_{1\mu}$, for both $p$ and $s$ polarizations of the incident light are given in Appendix A. In what follows the Hertz vectors associated with these fields are denoted by $\mathbf{\Phi}^\sigma_1$ ($\sigma = e,m$). Analogously one can find the reflected fields in the region $z < -L/2$. We denote the Hertz vectors associated with the fields at $z < -L/2$ in the absence of the hole by $\mathbf{\Phi}^\sigma_0$. These fields include the incident wave fields, $\mathbf{E}^i$ and $\mathbf{H}^i$, Eqs. (1) and (2), and together with the fields determined by the potentials $\mathbf{\Phi}^\sigma_1$ they satisfy the continuity of the tangential components at $z = -L/2$.

Let us consider now the film with a hole. To proceed we use a variant of the induction theorem formulated by Schelkunoff.[23] The presence of the hole both disturbs the fields below the entrance hole aperture leading to the "reflected" fields, $\mathbf{E}'$ and $\mathbf{H}'$, and produces the fields $\mathbf{E}''$ and $\mathbf{H}''$ above it. At this moment we do not know these fields, however; to find them in a first approximation we require that their components tangential to the plane $z = -L/2$ would be continuous across this plane, namely,

$$\mathbf{E}^-_{1t} + \mathbf{E}'^{(1)}_t = \mathbf{E}''^{(1)}_t, \tag{7}$$

$$\mathbf{H}^-_{1t} + \mathbf{H}'^{(1)}_t = \mathbf{H}''^{(1)}_t, \tag{8}$$

where the superscript minus sign means that the field components are taken at $z = -L/2$, the subscript $t$ denotes the components tangential to the film surface, and the superscript (1) designates the first approximation, which is corrected later. Here we have used the fact that in the absence of the hole the tangential field components are equal to $\mathbf{E}^-_{1t}$ and $\mathbf{H}^-_{1t}$ on both sides from the plane $z = -L/2$. According to Schelkunoff,[23] the field $\bar{\mathbf{E}}^{(1)}$, $\bar{\mathbf{H}}^{(1)}$ composed of $\mathbf{E}'^{(1)}$, $\mathbf{H}'^{(1)}$ below the plane $z = -L/2$ and of $\mathbf{E}''^{(1)}$, $\mathbf{H}''^{(1)}$ above it could be produced by electric and magnetic current sheets over the entrance hole aperture with the current densities

$$\mathbf{K}^e = \frac{c}{4\pi} \mathbf{e}_z \times \mathbf{H}^-_{1t} \tag{9}$$

and

$$\mathbf{K}^m = -\frac{c}{4\pi} \mathbf{e}_z \times \mathbf{E}^-_{1t}, \tag{10}$$

respectively [see Fig. 1(b)]. Using the expansion

$$e^{ik_{0x}x} = e^{ik_{0x}r\cos\theta} = \sum_{n=-\infty}^{\infty} i^n J_n(k_{0x}r) e^{-in\theta} \tag{11}$$

with $J_n(\rho)$ the Bessel function of the first kind, one can represent the current densities in the form

$$\mathbf{K}^{\sigma}(r,\theta) = \sum_{n=-\infty}^{\infty} \left[\kappa_{rn}^{\sigma}(r)\mathbf{e}_r + \kappa_{\theta n}^{\sigma}(r)\mathbf{e}_{\theta}\right] e^{-in\theta}, \tag{12}$$

where $\mathbf{e}_r$ and $\mathbf{e}_{\theta}$ are the unit vectors of the cylindrical coordinates and the current components $\kappa_{vn}^{\sigma}(r)$ depend on the incident wave polarization. In the following we consider in detail the case of light transmission through a hole in an optically thick metal film. This implies that the film thickness is much larger than the skin depth, i.e.,

$$L \gg (\mathrm{Im}k_1)^{-1}. \tag{13}$$

One can show that in this limit the contribution of the amplitudes $F_{-}^{\sigma}$ in Eqs. (A1)–(A10) can be neglected. In such a case the fictitious current components take the form given in Appendix B.

The Hertz vectors which describe the fields produced by the fictitious currents (9) and (10) in the hole interior can be found with the use of Green's function as follows:

$$\Phi_2^{\sigma}(\mathbf{R}) = \frac{i}{\tau_2^{\sigma}\omega}\int_{S_2} \mathbf{K}^{\sigma}(\mathbf{R}')\frac{e^{ik_2|\mathbf{R}-\mathbf{R}'|}}{|\mathbf{R}-\mathbf{R}'|}d\mathbf{R}', \tag{14}$$

where $\tau_j^e = \epsilon_j$, $\tau_j^m = 1$, the surface $S_2$ is the entrance opening of the hole, and it is assumed that the currents $\mathbf{K}^e$ and $\mathbf{K}^m$ are taken in the rectangular coordinates $(x,y,z)$.

The distance between the points $\mathbf{R}$ and $\mathbf{R}'$ can be written in the cylindrical coordinates as follows:

$$|\mathbf{R}-\mathbf{R}'| = \sqrt{d^2 + (z+L/2)^2} \tag{15}$$

with

$$d = \sqrt{r^2 + r'^2 - 2rr'\cos(\theta-\theta')}. \tag{16}$$

Now using the identity[24]

$$\frac{e^{ik_j\sqrt{d^2+z^2}}}{\sqrt{d^2+z^2}} = \frac{i}{2}\int_{-\infty}^{\infty} H_0^{(1)}(q_j d)e^{i\beta z}d\beta \tag{17}$$

and the theorem of addition for the cylindrical functions,

$$H_0^{(1)}(q_j d) = \sum_{s=-\infty}^{\infty} J_s(q_j r_<)H_s^{(1)}(q_j r_>)e^{-is(\theta-\theta')} \tag{18}$$

with

$$q_j = \sqrt{k_j^2 - \beta^2}, \quad 0 \leqslant \mathrm{Arg}(q_j) < \pi, \tag{19}$$

$r_< = \min(r,r')$, $r_> = \max(r,r')$, and $H_n^{(1)}(\rho)$ the Hankel function of the first kind, one can express the quantity (14) in the form of the Fourier integral over $\beta$. To include in the consideration any arbitrary values of $\beta$, we analytically continue the corresponding Fourier transform onto the whole complex plane of $\beta$ and take the integral over the integration path $C$, which runs along the real axis (see Fig. 2). As a result, we obtain

$$\Phi_2^{\sigma}(r,\theta,z) = \frac{1}{2\pi}\int_C \tilde{\Phi}_2^{\sigma}(r,\theta;\beta)e^{i\beta(z+L/2)}d\beta, \tag{20}$$

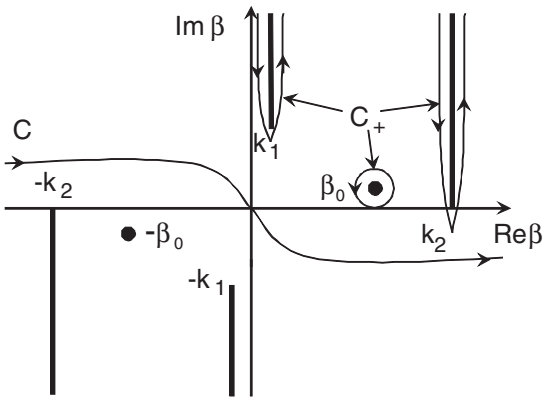


FIG. 2. Complex plane of the axial propagation constant, $\beta$. The cuts and poles are shown schematically by thick lines and dots, respectively. For simplicity, only a single waveguide mode, $\beta_0$, is indicated. The integration path $C_+$ includes also the arcs of an infinite radius.

where

$$\tilde{\Phi}_2^{\sigma} = \sum_{n=-\infty}^{\infty} \tilde{\Phi}_{2n}^{\sigma} e^{-in\theta} \tag{21}$$

with

$$\tilde{\Phi}_{2n}^{\sigma}(r;\beta) = -\frac{\pi^2}{\tau_2^{\sigma}\omega}\int_0^a \left[\mathbf{p}_{n-}^{\sigma}(r')J_{n-1}(q_2 r_<)H_{n-1}^{(1)}(q_2 r_>) + \mathbf{p}_{n+}^{\sigma}(r')J_{n+1}(q_2 r_<)H_{n+1}^{(1)}(q_2 r_>)\right]r'dr'. \tag{22}$$

Here the functions $\mathbf{p}_{n\pm}^{\sigma}(r)$ are defined as follows:

$$\mathbf{p}_{n\pm}^{\sigma}(r) = \left[\kappa_{rn}^{\sigma}(r) \mp i\kappa_{\theta n}^{\sigma}(r)\right](\mathbf{e}_r \pm i\mathbf{e}_{\theta}). \tag{23}$$

### C. Solution inside the film

Equations (20)–(22) give a partial solution of the Helmholtz equation which, being combined with the fields determined by the potentials $\mathbf{\Phi}_0^{\sigma}$, obeys the continuity of the tangential field components at $z = -L/2$ [see Eqs. (7) and (8)]. It does not, however, satisfy the necessary boundary conditions at the hole wall, $r = a$. To obtain a general solution for the fields in the slab $-L/2 < z < L/2$ we add to the Hertz vectors $\mathbf{\Phi}_j^{\sigma}$ a general solution of the homogeneous Helmholtz equation which only has a $z$ component, $\Psi_j^{\sigma}$,[21] so that the total Hertz vectors take the form

$$\mathbf{\Pi}_j^{\sigma} = \mathbf{\Phi}_j^{\sigma} + \Psi_j^{\sigma}\mathbf{e}_z, \quad j = 1,2. \tag{24}$$

The quantities $\Psi_j^{\sigma}$ can be written as the Fourier integrals

$$\Psi_j^{\sigma}(r,\theta,z) = \frac{1}{2\pi}\int_C \tilde{\Psi}_j^{\sigma}(r,\theta;\beta)e^{i\beta z}d\beta \tag{25}$$

with the same integration path $C$ as before. The Fourier transforms $\tilde{\Psi}_j^{\sigma}$ in their turn can be expanded in the elementary waves of a cylinder,

$$\tilde{\Psi}_j^{\sigma}(r,\theta;\beta) = \frac{1}{q_j^2}\sum_{n=-\infty}^{\infty} a_{jn}^{\sigma}(\beta)Z_n(q_j r)e^{-in\theta}, \tag{26}$$

where $Z_n(\rho)$ is a cylindrical function defined as

$$Z_n(q_j r) = \begin{cases} J_n(q_2 r) & \text{if } r < a, \\ H_n^{(1)}(q_1 r) & \text{if } r > a. \end{cases} \tag{27}$$

Due to the contributions given by the Hertz vectors $\mathbf{\Psi}_j^\sigma = \Psi_j^\sigma \mathbf{e}_z$, the boundary conditions for the total fields dictated by the Hertz vectors $\mathbf{\Pi}_j^\sigma$, Eq. (24), are not satisfied at both planes $z = -L/2$ and $z = L/2$. The discontinuities of the tangential field components at these surfaces can be represented by the fictitious electric and magnetic surface currents [see Fig. 1(b)] by the same procedure as in Sec. II B:

$$\mathbf{L}_j^{e\pm} = \frac{c}{4\pi} \mathbf{e}_z \times \mathbf{H}_j^{\psi\pm} \tag{28}$$

and

$$\mathbf{L}_j^{m\pm} = -\frac{c}{4\pi} \mathbf{e}_z \times \mathbf{E}_j^{\psi\pm}, \tag{29}$$

respectively, with

$$\mathbf{E}_j^{\psi\pm}(r,\theta) = \frac{1}{2\pi} \int_C \sum_{n=-\infty}^{\infty} [\tilde{E}_{jrn}^{\psi}(r;\beta)\mathbf{e}_r + \tilde{E}_{j\theta n}^{\psi}(r;\beta)\mathbf{e}_\theta] e^{-in\theta} e^{\pm i\beta L/2} d\beta, \tag{30}$$

$$\mathbf{H}_j^{\psi\pm}(r,\theta) = \frac{1}{2\pi} \int_C \sum_{n=-\infty}^{\infty} [\tilde{H}_{jrn}^{\psi}(r;\beta)\mathbf{e}_r + \tilde{H}_{j\theta n}^{\psi}(r;\beta)\mathbf{e}_\theta] e^{-in\theta} e^{\pm i\beta L/2} d\beta, \tag{31}$$

where the $\pm$ signs correspond to the planes $z = \pm L/2$ and the Fourier-transformed field components $\tilde{E}_{j\mu n}^{\psi}$ and $\tilde{H}_{j\mu n}^{\psi}$ are given in Appendix C.

The coefficients $a_{jn}^\sigma(\beta)$ in Eq. (26) are not yet defined. We choose them to ensure the continuity of the tangential components of the total fields across the cylindrical surface $r = a$. This field inside the hole ($j = 2$) and outside it ($j = 1$) is given by a sum of the fields originating from the Hertz vector $\mathbf{\Pi}_j$, Eq. (24), and the fields produced by the currents $\mathbf{L}_j^{\sigma\pm}$, Eqs. (28) and (29). As a result the boundary condition at $r = a$ is reduced to the integral equation

$$\hat{M}_n(\beta)\vec{A}_n(\beta) - \frac{1}{2\pi} \int_C [e^{-i(\beta-\beta')L/2} - e^{i(\beta-\beta')L/2}] \times \hat{N}_n(\beta,\beta')\vec{A}_n(\beta')d\beta' = \vec{B}_n(\beta)e^{i\beta L/2}, \tag{32}$$

where

$$\vec{A}_n(\beta) = \begin{pmatrix} a_{2n}^e(\beta) \\ a_{2n}^m(\beta) \\ a_{1n}^e(\beta) \\ a_{1n}^m(\beta) \end{pmatrix}, \tag{33}$$

and

$$\vec{B}_n(\beta) = \begin{pmatrix} \Delta\tilde{E}_{\theta n}(\beta) \\ \Delta\tilde{E}_{zn}(\beta) \\ \Delta\tilde{H}_{\theta n}(\beta) \\ \Delta\tilde{H}_{zn}(\beta) \end{pmatrix} \tag{34}$$

with $\Delta\tilde{E}_{\mu n}(\beta) \equiv \tilde{E}_{1\mu n}(a;\beta) - \tilde{E}_{2\mu n}^{\phi}(a;\beta)$ and $\Delta\tilde{H}_{\mu n}(\beta) \equiv \tilde{H}_{1\mu n}(a;\beta) - \tilde{H}_{2\mu n}^{\phi}(a;\beta)$, $\mu = \theta, z$; the tilde above a symbol denotes the Fourier transform of the corresponding quantity. The explicit form of the field amplitudes $\tilde{E}_{1\mu n}(r;\beta)$, $\tilde{H}_{1\mu n}(r;\beta)$ and $\tilde{E}_{2\mu n}^{\phi}(r;\beta)$, $\tilde{H}_{2\mu n}^{\phi}(r;\beta)$ as well as the matrices $\hat{M}_n(\beta)$ and $\hat{N}_n(\beta,\beta')$ are given in Appendices D, E, and F, respectively.

Let us note that the equation

$$\hat{M}_n(\beta)\vec{A}_n(\beta) = 0 \tag{35}$$

determines the solutions of source-free Maxwell equations for a cylindrical hole in an infinite metal. Correspondingly, the roots of $\det \hat{M}_n(\beta)$, $\beta_a$, specify the waveguide modes of such a channel. The quantity $\det \hat{M}_n(\beta)$ contains $\beta$ only in the form of $\beta^2$; therefore, both $\beta_a$ and $-\beta_a$ are the roots of $\det \hat{M}_n(\beta)$. The integral on the left-hand side of Eq. (32) originates from the contribution of the channel terminations. The nontrivial solutions of the homogeneous equation which corresponds to Eq. (32) give the normal modes of a hole in a metal film of finite thickness.[20]

## III. TRANSMITTED FIELD

The fields $\mathbf{E}_j^{\psi+}$ and $\mathbf{H}_j^{\psi+}$ along with the fields originating from the Hertz vectors $\mathbf{\Phi}_2^\sigma$ taken at $z = L/2$ dictate the electromagnetic field transmitted through the film. Denoting the latter contribution to the fictitious surface currents by $\mathbf{M}^\sigma$, one can write the Hertz vectors of the transmitted field as follows:

$$\mathbf{\Omega}^\sigma(\mathbf{R}) = \frac{i}{\tau_0^\sigma \omega} \left\{ \int_{S_1} \mathbf{L}_1^{\sigma+}(\mathbf{R}') \frac{e^{ik_0|\mathbf{R}-\mathbf{R}'|}}{|\mathbf{R}-\mathbf{R}'|} d\mathbf{R}' + \int_{S_2} [\mathbf{L}_2^{\sigma+}(\mathbf{R}') + \mathbf{M}^\sigma(\mathbf{R}')] \frac{e^{ik_0|\mathbf{R}-\mathbf{R}'|}}{|\mathbf{R}-\mathbf{R}'|} d\mathbf{R}' \right\}, \tag{36}$$

where the surfaces $S_1$ and $S_2$ are the back film surface and the exit opening of the hole, respectively.

Using identities (17) and (18), one can transform Eq. (36) to the form

$$\mathbf{\Omega}^\sigma(r,\theta,z) = \frac{1}{2\pi} \int_C \sum_{n=-\infty}^{\infty} [\tilde{\mathbf{\Omega}}_{1n}^\sigma(r;\beta) + \tilde{\mathbf{\Omega}}_{2n}^\sigma(r;\beta)] \times e^{-in\theta} e^{i\beta(z-L/2)} d\beta, \tag{37}$$

where

$$\tilde{\mathbf{\Omega}}_{jn}^\sigma(r;\beta) = -\frac{\pi^2}{\tau_0^\sigma \omega} \int_{A_j} [\mathbf{q}_{jn-}^\sigma(r') J_{n-1}(q_0 r_<) H_{n-1}^{(1)}(q_0 r_>) + \mathbf{q}_{jn+}^\sigma(r') J_{n+1}(q_0 r_<) H_{n+1}^{(1)}(q_0 r_>)] r' dr' \tag{38}$$

with

$$A_j = \begin{cases} [a,\infty) & \text{if } j = 1, \\ [0,a] & \text{if } j = 2, \end{cases} \tag{39}$$

$$\mathbf{q}_{1n\pm}^\sigma(r) = [\lambda_{1rn}^\sigma(r) \mp i\lambda_{1\theta n}^\sigma(r)](\mathbf{e}_r \pm i\mathbf{e}_\theta), \tag{40}$$

and

$$\mathbf{q}_{2n\pm}^\sigma(r) = \{[\lambda_{2rn}^\sigma(r) + \mu_{rn}^\sigma(r)] \mp i[\lambda_{2\theta n}^\sigma(r) + \mu_{\theta n}^\sigma(r)]\}(\mathbf{e}_r \pm i\mathbf{e}_\theta). \tag{41}$$

Here the quantities $\lambda^{\sigma}_{jrn}$, $\lambda^{\sigma}_{j\theta n}$ and $\mu^{\sigma}_{rn}$, $\mu^{\sigma}_{\theta n}$ are determined by the components of the fictitious currents $\mathbf{L}^{\sigma+}_{j}$ and $\mathbf{M}^{\sigma}$, respectively, and are given in Appendix G.

The Fourier transforms of the electromagnetic field amplitudes associated with the Hertz vectors $\mathbf{\Omega}^{\sigma}$ can be obtained formally from Eqs. (E3)–(E10) with the use of the following substitutions:

$$p^{\sigma}_{n\pm,r} \to q^{\sigma}_{jn\pm,r}, \quad \tau^{\sigma}_{j} \to \tau^{\sigma}_{0}, \quad q_j \to q_0. \tag{42}$$

The Hertz vectors of the transmitted field can be significantly simplified in the far-field region where $k_0 R \gg 1$ with $R = \sqrt{r^2 + (z - L/2)^2}$. Assuming also that $q_0 r \gg 1$, one can replace the Hankel functions by their asymptotics and come to the expression

$$\tilde{\mathbf{\Omega}}^{\sigma}_{jn}(r;\beta) \approx \frac{i\pi^{3/2}}{\omega}\sqrt{\frac{2}{q_0 r}}e^{-i(2n+1)\pi/4}[\mathbf{S}^{\sigma}_{jn+}(\beta) - \mathbf{S}^{\sigma}_{jn-}(\beta)]e^{iq_0 r}, \tag{43}$$

where

$$\mathbf{S}^{\sigma}_{jn\pm}(\beta) = \frac{1}{\tau^{\sigma}_{0}}\int_{A_j}\mathbf{q}^{\sigma}_{jn\pm}(r')J_{n\pm1}(q_0 r')r'dr'. \tag{44}$$

Substituting Eq. (43) in Eq. (37) and considering the distance to the observation point, $R$, as a large parameter, one can evaluate the Fourier integral with the use of the steepest-descent method. Introducing the angle of diffraction, $\chi$, by the relations

$$r = R\sin\chi, \quad z - L/2 = R\cos\chi, \tag{45}$$

one finds $\mathbf{\Omega}^{\sigma} = \mathbf{\Omega}^{\sigma}_{1} + \mathbf{\Omega}^{\sigma}_{2}$, where

$$\mathbf{\Omega}^{\sigma}_{j}(R,\chi,\theta) \approx \frac{\pi}{\omega}\frac{e^{ik_0 R}}{R}\mathbf{Q}^{\sigma}_{j}(\chi,\theta) \tag{46}$$

with

$$\mathbf{Q}^{\sigma}_{j}(\chi,\theta) = \sum_{n=-\infty}^{\infty}(-i)^n e^{-in\theta}[\mathbf{S}^{\sigma}_{jn+}(\beta_s) - \mathbf{S}^{\sigma}_{jn-}(\beta_s)] \tag{47}$$

and $\beta_s = k_0\cos\chi$ is the saddle point.

The electromagnetic field determined by the Hertz vectors (46) is purely transversal in the leading order in $1/R$; i.e., $E_R = H_R = 0$. The corresponding power diffracted into the elementary solid angle $d\Omega = \sin\chi d\chi d\theta$ is given by

$$dP(\chi,\theta) \approx \frac{\pi\omega^2\epsilon_0^{3/2}}{8c^3}(\mid G_{\chi}(\chi,\theta)\mid^2 + \mid G_{\theta}(\chi,\theta)\mid^2)d\Omega, \tag{48}$$

where the functions $G_{\chi}(\chi,\theta)$ and $G_{\theta}(\chi,\theta)$ determine the angular dependence of the field components $E_{\chi}$ and $E_{\theta}$, respectively. They are found as follows:

$$G_{\mu}(\chi,\theta) = \sum_{n=-\infty}^{\infty}(-i)^n e^{-in\theta}[G_{1\mu n}(\chi) + G_{2\mu n}(\chi)], \quad \mu = \chi,\theta \tag{49}$$

with

$$G_{j\chi n}(\chi) = \sqrt{\epsilon_0}\left[S^{e}_{jn+,r}(\beta_s) - S^{e}_{jn-,r}(\beta_s)\right]\cos\chi + i\left[S^{m}_{jn+,r}(\beta_s) + S^{m}_{jn-,r}(\beta_s)\right], \tag{50}$$

$$G_{j\theta n}(\chi) = i\sqrt{\epsilon_0}\left[S^{e}_{jn+,r}(\beta_s) + S^{e}_{jn-,r}(\beta_s)\right] - \left[S^{m}_{jn+,r}(\beta_s) - S^{m}_{jn-,r}(\beta_s)\right]\cos\chi, \tag{51}$$

and $S^{\sigma}_{jn\pm,r}$ are the $r$ components of the vectors $\mathbf{S}^{\sigma}_{jn\pm}$.

The total power transmitted through the film is given by

$$P = \int_0^{2\pi}\int_0^{\pi/2} dP(\chi,\theta) \approx \frac{\pi^2\omega^2\epsilon_0^{3/2}}{4c^3} \times \sum_{n=-\infty}^{\infty}\int_0^{\pi/2}[\mid G_{1\chi n}(\chi) + G_{2\chi n}(\chi)\mid^2 + \mid G_{1\theta n}(\chi) + G_{2\theta n}(\chi)\mid^2]\sin\chi d\chi, \tag{52}$$

where we have neglected the contribution of small diffraction angles such that $\chi \leqslant 1/\sqrt{k_0 R}$. Let us note that at normal incidence ($\alpha = 0$) the sum in Eq. (52) contains only the terms with $n = \pm 1$.

In just the same way as it has been done in this section one can find the field diffracted into the half-space $z < -L/2$. This field is determined by the fictitious currents $\mathbf{K}^{\sigma}$ and $\mathbf{L}^{\sigma-}_{j}$. In the far-field region where $q_0 r \gg 1$, its evanescent part can be represented by a cylindrical wave similar to (43) integrated over imaginary propagation constants $\beta$. This contribution varies with the distance from the hole center as $e^{ik_0 r}/r$. Such a diffracted field was invoked in Ref. 13 to explain light transmission through subwavelength hole arrays.

## IV. LIMIT OF ELONGATED HOLE

Up to this point we have not made any assumptions regarding the hole sizes. In this section we assume that the film thickness exceeds considerably the hole diameter; i.e., $L \gg 2a$. Let us rewrite Eq. (32) in the following form:

$$\vec{C}_n(\beta) - \frac{1}{2\pi}\left[\int_{C_+} e^{-i(\beta-\beta')L/2}\hat{N}_n(\beta,\beta')\hat{M}_n^{-1}(\beta')\vec{C}_n(\beta')d\beta' - \int_{C_-} e^{i(\beta-\beta')L/2}\hat{N}_n(\beta,\beta')\hat{M}_n^{-1}(\beta')\vec{C}_n(\beta')d\beta'\right] = \vec{B}_n(\beta)e^{i\beta L/2}, \tag{53}$$

where

$$\vec{C}_n(\beta) = \hat{M}_n(\beta)\vec{A}_n(\beta). \tag{54}$$

The integration path $C_+$ runs in the upper half-plane embracing the cuts and the poles in the right half-plane of the complex plane of $\beta$ (see Fig. 2) while the integration path $C_-$ runs similarly in the lower half-plane embracing the cuts and the poles in the left half-plane (not shown). The contributions from the cut edges are estimated as being of the order of $(2a/L)^2$ and can be neglected. The remaining integrals are determined by the sum of residues of the integrands at the poles given by the roots of $\det\hat{M}_n(\beta')$, i.e., by the propagation constants of the normal modes of an infinitely long hole, $\beta_a$. As a result, one comes to the

following equation:

$$\vec{C}_n(\beta) - i\Big\{\sum_b e^{-i(\beta-\beta_b)L/2}\hat{N}_n(\beta,\beta_b)\mathrm{Res}\big[\hat{M}_n^{-1}(\beta_b)\big]\vec{C}_n(\beta_b) + \sum_b e^{i(\beta+\beta_b)L/2}\hat{N}_n(\beta,-\beta_b) \times \mathrm{Res}\big[\hat{M}_n^{-1}(-\beta_b)\big]\vec{C}_n(-\beta_b)\Big\} = \vec{B}_n(\beta)e^{i\beta L/2}, \quad (55)$$

where $\mathrm{Res}[\hat{M}_n^{-1}(\beta_b)]$ is a matrix composed of the residues of the matrix elements of $\hat{M}_n^{-1}(\beta)$ at the pole $\beta=\beta_b$. Equation (55) determines the vector functions $\vec{C}_n(\beta)$ in terms of the vector coefficients $\vec{C}_n(\beta_b)$ which satisfy in their turn the set of equations

$$\vec{C}_n(\beta_a) - i\Big\{\sum_b e^{-i(\beta_a-\beta_b)L/2}\hat{N}_n(\beta_a,\beta_b)\mathrm{Res}\big[\hat{M}_n^{-1}(\beta_b)\big]\vec{C}_n(\beta_b) + \sum_b e^{i(\beta_a+\beta_b)L/2}\hat{N}_n(\beta_a,-\beta_b) \times \mathrm{Res}\big[\hat{M}_n^{-1}(-\beta_b)\big]\vec{C}_n(-\beta_b)\Big\} = \vec{B}_n(\beta_a)e^{i\beta_a L/2}. \quad (56)$$

The dimension of this set of equations is dictated by the number of waveguide modes which are supported by an infinitely long hole at a given frequency $\omega$ for a given number $n$, the modes propagating in both directions being taken into account.

In the considered limit the functions $\lambda^{\sigma}_{j\nu n}(r)$ and $\mu^{\sigma}_{\nu n}(r)$, $\nu = r,\theta$, which determine the fictitious surface currents at the exit hole opening, can also be significantly simplified. Replacing the path of integration, $C$, in Eqs. (G1)–(G8) by the contour $C_+$ and neglecting the contribution from the cut edges as before, one obtains that the functions $\lambda^{\sigma}_{j\nu n}(r)$ are reduced to the sum of the contributions from the poles $\beta_a$ of the coefficients $a^{\sigma}_{jn}(\beta)$ while all the functions $\mu^{\sigma}_{\nu n}(r)=0$. Taking into account the representation $\vec{A}_n(\beta)=\hat{M}_n^{-1}(\beta)\vec{C}_n(\beta)$, one concludes that the poles of the coefficients $a^{\sigma}_{jn}(\beta)$ are given by both the normal modes of an infinitely long hole, $\beta_a$, and the pole $\beta=k_{1z}$, which appears in the components of the vector function $\vec{B}(\beta)$. The latter pole gives the contribution to the quantities $\lambda^{\sigma}_{j\nu n}(r)$, which is proportional to the factor $\exp(ik_{1z}L)$ and hence can be neglected in the limit of an optically thick film.

Let us consider in some more detail the limit of a subwavelength hole when for a given $n$ only a single mode, $\beta_0$, gives an essential contribution to the field amplitudes. Then the vector coefficients $\vec{C}(\beta_0)$ satisfy the equation

$$\hat{\mathcal{O}}_n(\beta_0)\vec{\mathcal{C}}_n(\beta_0) = \vec{\mathcal{B}}_n(\beta_0) \quad (57)$$

with

$$\vec{\mathcal{C}}_n(\beta) = \begin{pmatrix}\vec{C}_n(\beta)\\ \vec{C}_n(-\beta)\end{pmatrix} \quad (58)$$

and

$$\vec{\mathcal{B}}_n(\beta) = \begin{pmatrix}\vec{B}_n(\beta)e^{i\beta L/2}\\ \vec{B}_n(-\beta)e^{-i\beta L/2}\end{pmatrix}. \quad (59)$$

Here $\hat{\mathcal{O}}_n(\beta)$ is a block matrix

$$\hat{\mathcal{O}}_n(\beta) = \begin{pmatrix}\hat{O}_{n,11}(\beta) & \hat{O}_{n,12}(\beta)\\ \hat{O}_{n,21}(\beta) & \hat{O}_{n,22}(\beta)\end{pmatrix} \quad (60)$$

with

$$\hat{O}_{n,11}(\beta) = \hat{I} - i\hat{N}_n(\beta,\beta)\mathrm{Res}\big[\hat{M}_n^{-1}(\beta)\big], \quad (61)$$

$$\hat{O}_{n,12}(\beta) = -ie^{i\beta L}\hat{N}_n(\beta,-\beta)\mathrm{Res}\big[\hat{M}_n^{-1}(-\beta)\big], \quad (62)$$

$$\hat{O}_{n,21}(\beta) = -ie^{i\beta L}\hat{N}_n(-\beta,\beta)\mathrm{Res}\big[\hat{M}_n^{-1}(\beta)\big], \quad (63)$$

$$\hat{O}_{n,22}(\beta) = \hat{I} - i\hat{N}_n(-\beta,-\beta)\mathrm{Res}\big[\hat{M}_n^{-1}(-\beta)\big], \quad (64)$$

and $\hat{I}$ is a $4\times 4$ unit matrix. Let us note that the maxima of $|\det\hat{\mathcal{O}}_n(\beta_0)|^{-1}$ which can occur at certain $\omega$ determine the Fabry-Pérot modes of the nanohole (cf. Ref. 20).

The above equations can be further simplified if the waveguide mode decays essentially at the hole length; i.e., $\exp(-\mathrm{Im}\beta_0 L)\ll 1$. In such a case the equations for the vector coefficients $\vec{C}(\beta_0)$ and $\vec{C}(-\beta_0)$ are decoupled. Then the transmitted power normalized to the incident wave power through an area $\pi a^2$, $P_0$, takes the form

$$\frac{P}{P_0} = f(a,\lambda)e^{-2\mathrm{Im}\beta_0 L}, \quad (65)$$

where the coefficient $f(a,\lambda)$ does not depend on $L$.

## V. NUMERICAL RESULTS

We illustrate the general theory developed above by the numerical calculations of light transmission through a hole in an optically thick Ag film which was investigated experimentally in Ref. 3. To calculate the dielectric function of Ag we use the interpolation of the data represented in Ref. 25. For the case of normal incidence of light, one needs to take into account only the waveguide modes with $n=\pm 1$. Figure 3 shows the dispersion of such modes in the wavelength range of interest. It is seen that one of these modes is propagating below cutoff at $\lambda\approx 600$ nm and evanescent above it, while the other two modes are strongly evanescent in the whole considered domain. We use therefore the approximation of the elongated hole in the single-mode regime. The total power, $P$, transmitted through the hole calculated with the use of Eq. (52) and normalized to the quantity $P_0$ is represented in Fig. 4. The intensity drop at $\lambda\approx 600$ nm corresponds to the transition across the cutoff. This decrease is more sharp for a larger film thickness that is in agreement with the tendency observed in Ref. 3. One should keep in mind, however, that the approximation developed in Sec. IV is valid only for large aspect ratios, $L/(2a)\gg 1$.

The transmission spectra display also several distinct peaks whose positions differ for different hole depths. To elucidate their origin we have plotted the quantity $|\det\hat{\mathcal{O}}_n(\beta_0)|^{-1}$ in Fig. 5. One can see that the positions of the maxima in this figure exactly coincide with those in Fig. 4, which allows one to conclude that they correspond to the Fabry-Pérot modes of the nanohole.

Another feature which requires an explanation is the high intensity of the peaks ($P/P_0\geqslant 10$) near the cutoff wavelength. To understand this behavior we notice that in the considered

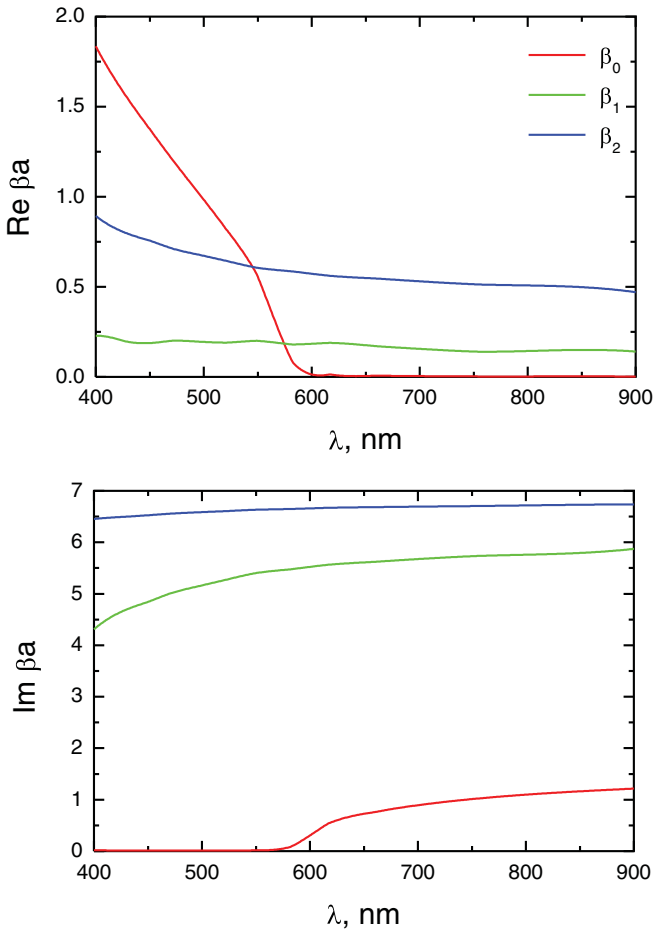


FIG. 3. (Color online) Dispersion of the waveguide modes with $n = \pm 1$ calculated for a hole of radius $a = 135$ nm in an Ag film; $\epsilon_2 = 1$.

approximation the field amplitudes are determined by the residues of the vector $\vec{A}_n(\beta)$ at the pole $\beta = \beta_0$:

$$\mathrm{Res}[\vec{A}_n(\beta_0)] = \mathrm{Res}\left[\hat{M}_n^{-1}(\beta_0)\right]\vec{C}_n(\beta_0), \tag{66}$$

where the matrix elements of the matrix $\mathrm{Res}[\hat{M}_n^{-1}(\beta_0)]$ are inversely proportional to the derivative $d[\det \hat{M}_n(\beta)]/d\beta$ taken at $\beta = \beta_0$. The latter quantity for $n = 1$ is plotted in Fig. 6. One can see that in the range $\lambda = 550$–$600$ nm both its real and imaginary parts are very close to zero, which explains the large amplitudes of the transmitted field. Such peculiar behavior is a consequence of the quasidegeneracy of the waveguide modes in the considered wavelength domain, which is seen in Fig. 3. Really, the expansion of the function $\det \hat{M}_1(\beta)$ in the vicinity of the point $\beta = \beta_0$ has the form

$$\det \hat{M}_1(\beta) = \det \hat{M}_1(\beta_0) + \left\{\frac{d[\det \hat{M}_1(\beta)]}{d\beta}\right\}_{\beta=\beta_0}(\beta - \beta_0) + \frac{1}{2}\left\{\frac{d^2[\det \hat{M}_1(\beta)]}{d\beta^2}\right\}_{\beta=\beta_0}(\beta - \beta_0)^2 + \cdots, \tag{67}$$

where $\det \hat{M}_1(\beta_0) = 0$ by the definition of a waveguide mode. On the other hand, the existence of a double root at $\beta = \beta_0$

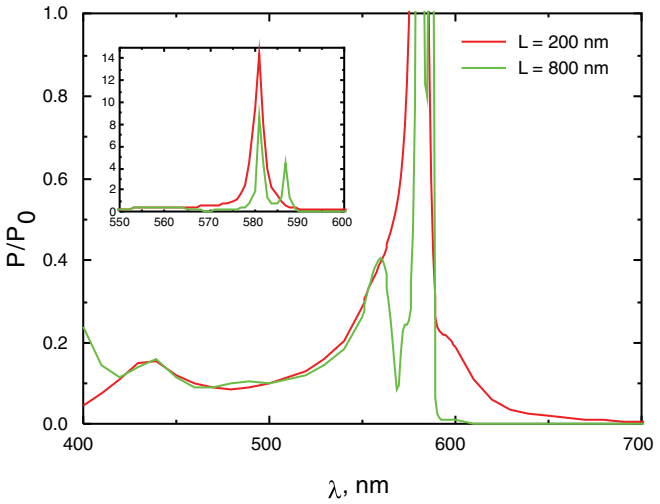


FIG. 4. (Color online) The normalized power transmitted through a hole in an Ag film; $\epsilon_0 = \epsilon_2 = 1$, $a = 135$ nm. Inset: the same quantity shown on a larger scale.

means that this expansion starts from the third term, which implies that $\{d[\det \hat{M}_n(\beta)]/d\beta\}_{\beta=\beta_0} = 0$.

Figure 7 illustrates the angular dependence of the transmitted light intensity in the far zone. One can see that for small diffraction angles ($|\chi| \leqslant 15^\circ$) the intensity almost does not depend on the angle $\theta$ which specifies the observation direction with respect to the plane of polarization of the incident wave. On the contrary, along the direction parallel to the film surface, the intensity differs sufficiently between scattering in the plane of polarization and perpendicularly to it.

Finally, Fig. 8 shows the dependence of the factor $f(a,\lambda)$ which determines the transmitted power in the limit of the infinite film thickness [see Eq. (65)] on the ratio $a/\lambda$ as compared with that calculated in the model of a perfectly conducting film.[12] The latter quantity is proportional to $(a/\lambda)^4$, so it is represented by a straight line on a double logarithmic scale. One can see that even in the limit of a subwavelength hole ($a \ll \lambda$) the power transmitted through a real metal film does not follow a power law with respect to $a/\lambda$. Its behavior is determined by the waveguide mode dispersion $\beta_0(\lambda)$. Also, it is seen that the model of a perfect conductor overestimates this quantity several-fold.

## VI. DISCUSSION

One of the purposes of the present paper is to elucidate the role of surface plasmon polaritons in light transmission through a hole in a real metal film. Although some authors, analyzing the numerical or experimental results on the EOT through an isolated hole, declare that SPPs participate in the transfer of energy through a hole, this statement requires a rigorous justification.

A surface plasmon polariton manifests itself as a pole in the Fourier (or Laplace) transform of the Hertz vector with respect to the wave-vector component parallel to the surface.[26] Its frequency dependence is given by the SPP dispersion relation. The contribution of this pole to the integral representation of the Hertz vector describes a SPP propagating along the surface. In this paper, we have found the Hertz vector of

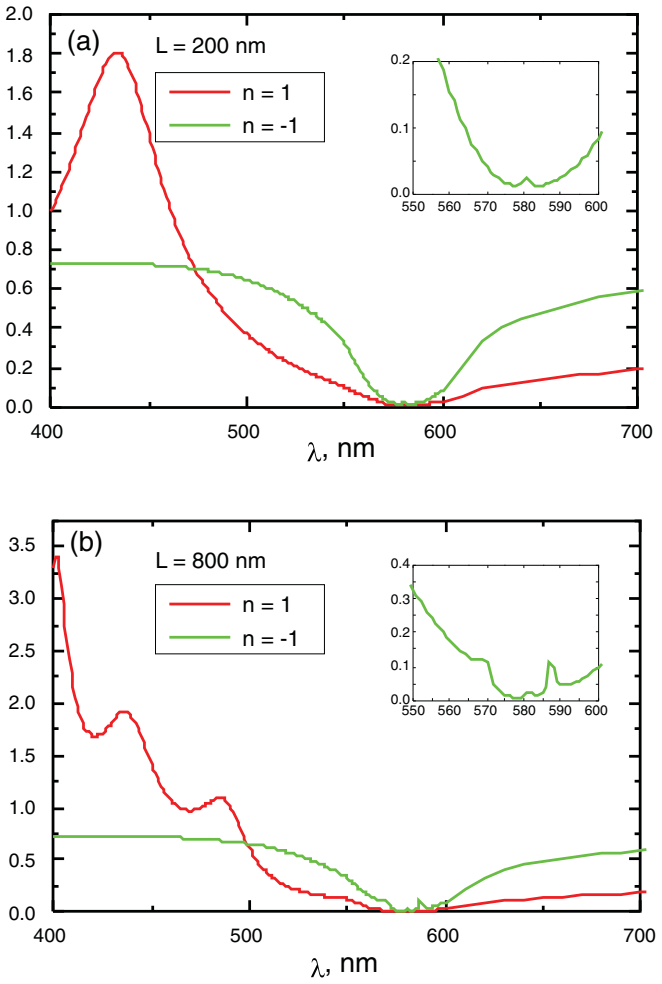


FIG. 5. (Color online) The wavelength dependence of the quantity $|\det \hat{\mathcal{O}}_n(\beta_0)|^{-1}$ for $n = \pm 1$. The maxima correspond to the Fabry-Pérot modes of the nanohole. Calculations for an Ag film, $\epsilon_0 = \epsilon_2 = 1$, $a = 135$ nm: (a) $L = 200$nm, (b) $L = 800$ nm. Insets: the same quantities shown in a narrow wavelength range.

the electromagnetic field transmitted through a cylindrical hole in a parallel plate of a real metal starting from first principles and not making any simplifying assumptions. We should emphasize that a pole which corresponds to a SPP does not appear in the Hertz vector Fourier transform. Instead, the transmitted electromagnetic field is governed by the normal modes of a finite-length hole. Such modes are determined by the solutions of the integral Eq. (32) with a zero right-hand-side part. They depend on the hole length, $L$, and can be identified with Fabry-Pérot modes of the hole.

In this context, it is necessary to stress that the light transmission through a subwavelength hole is a diffraction problem, and the normalization of the transmitted power to the incident wave power in the ray approximation may be somewhat misleading. In particular, the values of transmission efficiency exceeding unity do not necessarily mean that the field enhancement takes place. From this point of view, it is not surprising that the models which treat a metal as a perfect conductor are able to describe the extraordinary optical transmission.

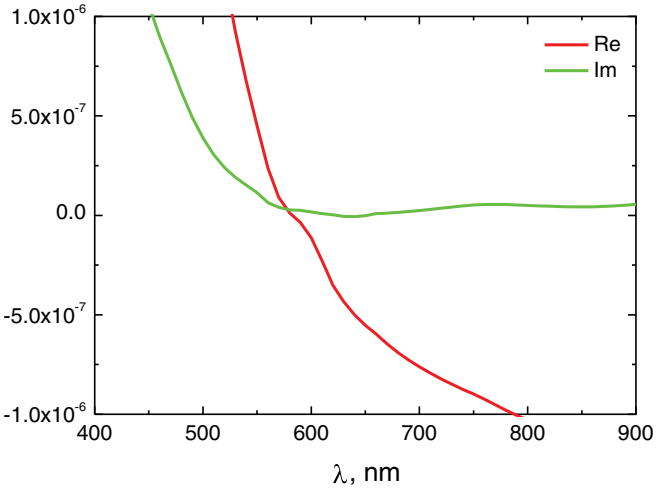


FIG. 6. (Color online) The wavelength dependence of the real and imaginary parts of the quantity $\{d[\det \hat{M}_1(\beta)]/d(\beta a)\}_{\beta=\beta_0}$. Calculations for an Ag film, $\epsilon_2 = 1$, $a = 135$ nm.

This does not exclude, however, that SPPs can be observed in experiments on light transmission through a nanohole. The authors of Ref. 27 have reported SPP generation from isolated nanoholes at the back side of an Au film. A source for such surface waves could be surface defects at the rim of the exit hole opening,[28] which are not considered in the framework of the present model. This process can be described in terms of an effective point dipole located *above* the surface (including the limit of an infinitesimal height above the surface). It is essentially the same model as that considered by Sommerfeld,[26] which involves excitation of SPPs. Alternatively, one can treat this problem using Green's dyadic functions. Such an approach has been used in Ref. 29 to find the surface electromagnetic field radiated by a hole in a metal film. The radiation from a hole itself, however, should be described by an effective dipole (or by fictitious surface currents as in the present paper) located *in* the surface plane. This case requires a special consideration since Green's dyadic

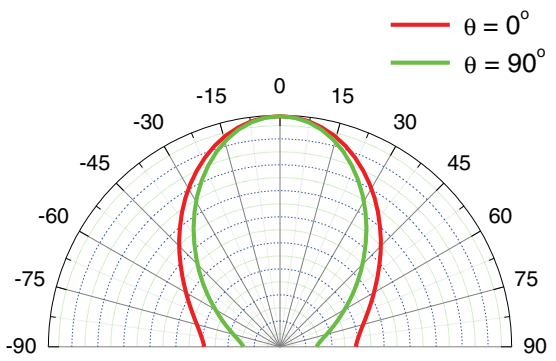


FIG. 7. (Color online) The angular dependence of the transmitted field intensity in the far zone for two different azimuthal angles, $\theta$. Calculations for an Ag film, $\epsilon_0 = \epsilon_2 = 1$, $a = 135$ nm, $L = 800$ nm, $\lambda = 581$ nm.

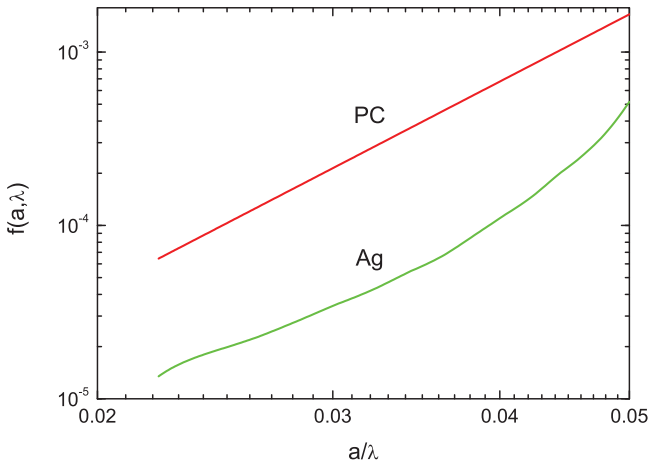


FIG. 8. (Color online) The dependence of the function $f(a,\lambda)$ [Eq. (65)] on the ratio $a/\lambda$ calculated for a hole of radius $a =$ 20 nm in an Ag film, double logarithmic scale. This factor found in the model of a perfectly conducting film is also shown for comparison.

as a function of the dipole position is discontinuous across the surface plane.

The question can arise of how the theory presented here correlates with the previous models. The only model which allows a rigorous analytical approach and can be found in the literature is that of a perfectly conducting film. One could try to obtain this limit by setting formally $\epsilon_1 \to i\infty$. In such a case the fictitious magnetic current $\mathbf{K}^m$, Eq. (10), is equal to zero while the fictitious electric current $\mathbf{K}^e$, Eq. (9), is nonzero. The latter current generates four nonzero tangential field components ($E_\theta$, $E_z$, $H_\theta$, and $H_z$) at the cylindrical hole surface $r = a$. However, the general solution of the homogeneous Helmholtz equation for a hole in a PC film for a given $n$ is determined by only two arbitrary constants, $a^e_{2n}$ and $a^m_{2n}$, because the fields outside the hole are identically equal to zero. The set of four equations which follows from the boundary conditions is overdetermined in this case and it is not possible to find the Hertz vector in the form (24). Alternatively, one can conclude that the matrix $\hat{M}_n(\beta)$ becomes singular for a PC film and the developed approach does not allow a continuous limiting transition to this model.

## VII. CONCLUSION

In this paper, we have found an analytical solution of Maxwell's equations for a cylindrical hole of arbitrary size in a film of optically thick material. Having introduced fictitious surface current sheets at both film surfaces, we have satisfied the necessary conditions at all boundaries. The solution is found in the form of the Fourier integral over the axial component of the wave vector. We have derived the integral equation which determines the field-amplitude Fourier transforms. This general solution has been analyzed in the case when the hole length is considerably larger than its diameter. Then the integral equation is reduced to a set of linear algebraic equations whose dimension is dictated by the number of waveguide modes supported by a hole of a given diameter. We have illustrated the developed theory by the calculations of the transmission spectrum of a subwavelength hole in an optically thick Ag film. We have demonstrated that all spectral features can be clearly associated with the normal modes of the system. We have emphasized that surface plasmon polaritons, whose existence would be manifested as a specific pole in the field-amplitude Fourier transforms, do not appear in our analysis.

## APPENDIX A: FIELD AMPLITUDES INSIDE A FILM WITHOUT A HOLE

The field amplitudes depend on the polarization of the incident wave. For $p$ polarization,

$$E_{1x}(x,z) = k_{1z}\left(F^e_- e^{-ik_{1z}z} - F^e_+ e^{ik_{1z}z}\right)e^{ik_{0x}x}, \tag{A1}$$

$$E_{1y}(x,z) = 0, \tag{A2}$$

$$E_{1z}(x,z) = k_{0x}\left(F^e_- e^{-ik_{1z}z} + F^e_+ e^{ik_{1z}z}\right)e^{ik_{0x}x}, \tag{A3}$$

$$H_{1x}(x,z) = H_{1z}(x,z) = 0, \tag{A4}$$

$$H_{1y}(x,z) = -\epsilon_1\frac{\omega}{c}\left(F^e_- e^{-ik_{1z}z} + F^e_+ e^{ik_{1z}z}\right)e^{ik_{0x}x}. \tag{A5}$$

For $s$ polarization,

$$E_{1x}(x,z) = E_{1z}(x,z) = 0, \tag{A6}$$

$$E_{1y}(x,z) = \frac{\omega}{c}\left(F^m_- e^{-ik_{1z}z} - F^m_+ e^{ik_{1z}z}\right)e^{ik_{0x}x}, \tag{A7}$$

$$H_{1x}(x,z) = k_{1z}\left(F^m_- e^{-ik_{1z}z} - F^m_+ e^{ik_{1z}z}\right)e^{ik_{0x}x}, \tag{A8}$$

$$H_{1y}(x,z) = 0, \tag{A9}$$

$$H_{1z}(x,z) = k_{0x}\left(F^m_- e^{-ik_{1z}z} + F^m_+ e^{ik_{1z}z}\right)e^{ik_{0x}x}. \tag{A10}$$

Here

$$F^\sigma_\pm = -\frac{2ck_{0z}}{\omega}\frac{B^\sigma_\pm}{D^\sigma}e^{-i(k_{0z}\pm k_{1z})L/2} \tag{A11}$$

with $k_{1z} = \sqrt{k_1^2 - k_{0x}^2}$ and

$$B^e_\pm = (\epsilon_0 k_{1z} \pm \epsilon_1 k_{0z})H_0, \tag{A12}$$

$$B^m_\pm = (k_{1z} \pm k_{0z})E_0, \tag{A13}$$

$$D^e = (\epsilon_1 k_{0z} - \epsilon_0 k_{1z})^2 e^{ik_{1z}L} - (\epsilon_1 k_{0z} + \epsilon_0 k_{1z})^2 e^{-ik_{1z}L}, \tag{A14}$$

$$D^m = (k_{0z} - k_{1z})^2 e^{ik_{1z}L} - (k_{0z} + k_{1z})^2 e^{-ik_{1z}L}. \tag{A15}$$

## APPENDIX B: FICTITIOUS CURRENT COMPONENTS $\kappa^\sigma_{\mu n}$

The fictitious current amplitudes, $\kappa^\sigma_{\mu n}$, defined by Eq. (12) for an optically thick film are found for $p$ polarization of the incident wave as follows:

$$\kappa^e_{rn}(r) = \frac{i^{n-1}}{4\pi}\epsilon_1\omega A^e J_n'(k_{0x}r), \tag{B1}$$

$$\kappa^e_{\theta n}(r) = -\frac{i^n n}{4\pi}\frac{\epsilon_1\omega A^e}{k_{0x}r}J_n(k_{0x}r), \tag{B2}$$

$$\kappa^m_{rn}(r) = \frac{i^n n}{4\pi}\frac{ck_{1z}A^e}{k_{0x}r}J_n(k_{0x}r), \tag{B3}$$

$$\kappa^m_{\theta n}(r) = \frac{i^{n-1}}{4\pi}ck_{1z}A^e J_n'(k_{0x}r), \tag{B4}$$

where

$$A^e = \frac{2cH_0}{\omega}\frac{k_{0z}}{\epsilon_1 k_{0z}+\epsilon_0 k_{1z}}e^{-ik_{0z}L/2} \tag{B5}$$

and the prime above the Bessel function denotes its derivative with respect to its argument.

For $s$ polarization of the incident wave one finds

$$\kappa^e_{rn}(r) = -\frac{i^n n}{4\pi}\frac{ck_{1z}A^m}{k_{0x}r}J_n(k_{0x}r), \tag{B6}$$

$$\kappa^e_{\theta n}(r) = -\frac{i^{n-1}}{4\pi}ck_{1z}A^m J_n'(k_{0x}r), \tag{B7}$$

$$\kappa^m_{rn}(r) = -\frac{i^{n-1}}{4\pi}\omega A^m J_n'(k_{0x}r), \tag{B8}$$

$$\kappa^m_{\theta n}(r) = \frac{i^n n}{4\pi}\frac{\omega A^m}{k_{0x}r}J_n(k_{0x}r), \tag{B9}$$

where

$$A^m = \frac{2cE_0}{\omega}\frac{k_{0z}}{k_{0z}+k_{1z}}e^{-ik_{0z}L/2}. \tag{B10}$$

In the case of normal incidence $\alpha = 0$, $k_{0x} = 0$ and both polarizations are equivalent to each other. Then the sum (12) only contains the terms with $n = \pm 1$, and their cylindrical components are given by ($\mathbf{E}_0 \parallel \mathbf{e}_x$)

$$\kappa^e_{r,\pm1} = \frac{1}{8\pi}\epsilon_1\omega A^e_0, \tag{B11}$$

$$\kappa^e_{\theta,\pm1} = \mp\frac{i}{8\pi}\epsilon_1\omega A^e_0, \tag{B12}$$

$$\kappa^m_{r,\pm1} = \pm\frac{i}{8\pi}ck_1 A^e_0, \tag{B13}$$

$$\kappa^m_{\theta,\pm1} = \frac{1}{8\pi}ck_1 A^e_0 \tag{B14}$$

with

$$A^e_0 = \frac{2cH_0}{\omega}\frac{k_0}{\epsilon_1 k_0+\epsilon_0 k_1}e^{-ik_0L/2}. \tag{B15}$$

## APPENDIX C: FIELD AMPLITUDES ASSOCIATED WITH THE HERTZ VECTORS $\Psi^\sigma_j$

The field amplitudes dictated by the Hertz vectors $\mathbf{\Psi}^\sigma_j$ are obtained by their substitution in Eqs. (5) and (6) instead of the vectors $\Pi^\sigma_j$. The result has the form of the Fourier integrals

$$F^\psi_{j\mu}(r,\theta,z) = \frac{1}{2\pi}\int_C\sum_{n=-\infty}^{\infty}\tilde F^\psi_{j\mu n}(r;\beta)e^{-in\theta}e^{i\beta z}d\beta, \tag{C1}$$

with the Fourier-transformed quantities $\tilde F^\psi_{j\mu n}$ given by the following equations:

$$\tilde E^\psi_{jrn}(r;\beta) = \frac{i\beta}{q_j}Z_n'(q_jr)a^e_{jn}(\beta) + \frac{\omega n}{cq_j^2 r}Z_n(q_jr)a^m_{jn}(\beta), \tag{C2}$$

$$\tilde E^\psi_{j\theta n}(r;\beta) = \frac{\beta n}{q_j^2 r}Z_n(q_jr)a^e_{jn}(\beta) - \frac{i\omega}{cq_j}Z_n'(q_jr)a^m_{jn}(\beta), \tag{C3}$$

$$\tilde E^\psi_{jzn}(r;\beta) = Z_n(q_jr)a^e_{jn}(\beta), \tag{C4}$$

$$\tilde H^\psi_{jrn}(r;\beta) = -\frac{ck_j^2 n}{\omega q_j^2 r}Z_n(q_jr)a^e_{jn}(\beta) + \frac{i\beta}{q_j}Z_n'(q_jr)a^m_{jn}(\beta), \tag{C5}$$

$$\tilde H^\psi_{j\theta n}(r;\beta) = \frac{ick_j^2}{\omega q_j}Z_n'(q_jr)a^e_{jn}(\beta) + \frac{\beta n}{q_j^2 r}Z_n(q_jr)a^m_{jn}(\beta), \tag{C6}$$

$$\tilde H^\psi_{jzn}(r;\beta) = Z_n(q_jr)a^m_{jn}(\beta). \tag{C7}$$

Here the functions $Z_n$ are defined by Eq. (27) and the quantities $a^\sigma_{jn}$ are the coefficients in Eq. (26).

## APPENDIX D: FOURIER TRANSFORMS OF THE FIELDS TRANSMITTED INTO THE FILM

In the limit of an optically thick film one can neglect the coefficients $F^\sigma_-$ in Eqs. (A1)–(A10) and represent the $z$ dependence of the fields as follows:

$$e^{ik_{1z}(z+L/2)} = \frac{1}{2\pi i}\int_C\frac{e^{i\beta(z+L/2)}}{\beta-k_{1z}}d\beta. \tag{D1}$$

Then using expansion (11) one can write the cylindrical components of the field amplitudes in the form

$$F_{1\nu}(r,\theta,z) = \frac{1}{2\pi}\int_C\tilde F_{1\nu}(r,\theta;\beta)e^{i\beta(z+L/2)}d\beta, \tag{D2}$$

with

$$\tilde F_{1\nu}(r,\theta;\beta) = \sum_{n=-\infty}^{\infty}\tilde F_{1\nu n}(r;\beta)e^{-in\theta}. \tag{D3}$$

For $p$ polarization of the incident light, one obtains

$$\tilde E_{1rn}(r;\beta) = \frac{i^n k_{1z}A^e}{\beta-k_{1z}}J_n'(k_{0x}r), \tag{D4}$$

$$\tilde E_{1\theta n}(r;\beta) = \frac{i^{n-1}nk_{1z}A^e}{k_{0x}r(\beta-k_{1z})}J_n(k_{0x}r), \tag{D5}$$

$$\tilde H_{1rn}(r;\beta) = \frac{i^{n-1}n\epsilon_1\omega A^e}{ck_{0x}r(\beta-k_{1z})}J_n(k_{0x}r), \tag{D6}$$

$$\tilde H_{1\theta n}(r;\beta) = \frac{i^n\epsilon_1\omega A^e}{c(\beta-k_{1z})}J_n'(k_{0x}r). \tag{D7}$$

For $s$ polarization,

$$\tilde E_{1rn}(r;\beta) = -\frac{i^{n-1}n\omega A^m}{ck_{0x}r(\beta-k_{1z})}J_n(k_{0x}r), \tag{D8}$$

$$\tilde E_{1\theta n}(r;\beta) = \frac{i^n\omega A^m}{c(\beta-k_{1z})}J_n'(k_{0x}r), \tag{D9}$$

$$\tilde H_{1rn}(r;\beta) = \frac{i^n k_{1z}A^m}{\beta-k_{1z}}J_n'(k_{0x}r), \tag{D10}$$

$$\tilde H_{1\theta n}(r;\beta) = \frac{i^{n-1}nk_{1z}A^m}{k_{0x}r(\beta-k_{1z})}J_n(k_{0x}r). \tag{D11}$$

Here the quantities $A^\sigma$ are defined in Appendix B.

In the case of normal incidence ($\mathbf{E}_0 \parallel \mathbf{e}_x$), the only nonzero field components are those with $n = \pm 1$. They are given by

$$\tilde{E}_{1r,-1}(\beta) = \tilde{E}_{1r,1}(\beta) = \frac{ik_1 A_0^e}{2(\beta - k_1)}, \tag{D12}$$

$$\tilde{E}_{1\theta,-1}(\beta) = -\tilde{E}_{1\theta,1}(\beta) = -\frac{k_1 A_0^e}{2(\beta - k_1)}, \tag{D13}$$

$$\tilde{H}_{1r,-1}(\beta) = -\tilde{H}_{1r,1}(\beta) = -\frac{\epsilon_1 \omega A_0^e}{2c(\beta - k_1)}, \tag{D14}$$

$$\tilde{H}_{1\theta,-1}(\beta) = \tilde{H}_{1\theta,1}(\beta) = \frac{i\epsilon_1 \omega A_0^e}{2c(\beta - k_1)}, \tag{D15}$$

where $A_0^e$ is defined by Eq. (B15).

## APPENDIX E: FIELD AMPLITUDES ASSOCIATED WITH THE HERTZ VECTORS $\mathbf{\Phi}_2^\sigma$

The field components associated with the Hertz vectors $\mathbf{\Phi}_2^\sigma$ can be written as the Fourier integrals

$$F_{2\nu}^\phi(r,\theta,z) = \frac{1}{2\pi}\int_C \tilde{F}_{2\nu}^\phi(r,\theta;\beta) e^{i\beta(z+L/2)} d\beta, \tag{E1}$$

with

$$\tilde{F}_{2\nu}^\phi(r,\theta;\beta) = \sum_{n=-\infty}^{\infty} \tilde{F}_{2\nu n}^\phi(r;\beta) e^{-in\theta}, \tag{E2}$$

where the quantities $\tilde{F}_{2\nu n}^\phi$ are given by the equations

$$\begin{aligned}\tilde{E}_{2rn}^\phi(r;\beta) = -\frac{\pi^2}{\omega}\Bigg[&\beta\left(\beta P_{n<}^e - i\frac{\omega}{c}P_{n<}^m\right)H_{n-1}^{(1)}(q_2 r) + \beta\left(\beta P_{n>}^e - i\frac{\omega}{c}P_{n>}^m\right)J_{n-1}(q_2 r)\\ &+\beta\left(\beta Q_{n<}^e + i\frac{\omega}{c}Q_{n<}^m\right)H_{n+1}^{(1)}(q_2 r) + \beta\left(\beta Q_{n>}^e + i\frac{\omega}{c}Q_{n>}^m\right)J_{n+1}(q_2 r)\\ &+\frac{nq_2}{r}\left(P_{n<}^e + Q_{n<}^e\right)H_n^{(1)}(q_2 r) + \frac{nq_2}{r}\left(P_{n>}^e + Q_{n>}^e\right)J_n(q_2 r) + \frac{2i}{\pi\tau_2^e}\left(p_{n-,r}^e + p_{n+,r}^e\right)\Bigg],\end{aligned} \tag{E3}$$

$$\begin{aligned}\tilde{E}_{2\theta n}^\phi(r;\beta) = \frac{\pi^2}{\omega}\Bigg[&\left(ik_2^2 P_{n<}^e + \beta\frac{\omega}{c}P_{n<}^m\right)H_{n-1}^{(1)}(q_2 r) + \left(ik_2^2 P_{n>}^e + \beta\frac{\omega}{c}P_{n>}^m\right)J_{n-1}(q_2 r) - \left(ik_2^2 Q_{n<}^e - \beta\frac{\omega}{c}Q_{n<}^m\right)H_{n+1}^{(1)}(q_2 r)\\ &-\left(ik_2^2 Q_{n>}^e - \beta\frac{\omega}{c}Q_{n>}^m\right)J_{n+1}(q_2 r) - i\frac{nq_2}{r}\left(P_{n<}^e - Q_{n<}^e\right)H_n^{(1)}(q_2 r) - i\frac{nq_2}{r}\left(P_{n>}^e - Q_{n>}^e\right)J_n(q_2 r)\Bigg],\end{aligned} \tag{E4}$$

$$\tilde{E}_{2zn}^\phi(r;\beta) = \frac{\pi^2}{\omega}q_2\left\{\left[i\beta\left(P_{n<}^e - Q_{n<}^e\right) + \frac{\omega}{c}\left(P_{n<}^m + Q_{n<}^m\right)\right]H_n^{(1)}(q_2 r) + \left[i\beta\left(P_{n>}^e - Q_{n>}^e\right) + \frac{\omega}{c}\left(P_{n>}^m + Q_{n>}^m\right)\right]J_n(q_2 r)\right\}. \tag{E5}$$

Here the following functions have been introduced:

$$P_{n<}^\sigma(r) = \frac{1}{\tau_2^\sigma}\int_0^r p_{n-,r}^\sigma(r') J_{n-1}(q_2 r') r' dr', \tag{E6}$$

$$P_{n>}^\sigma(r) = \frac{1}{\tau_2^\sigma}\int_r^a p_{n-,r}^\sigma(r') H_{n-1}^{(1)}(q_2 r') r' dr', \tag{E7}$$

$$Q_{n<}^\sigma(r) = \frac{1}{\tau_2^\sigma}\int_0^r p_{n+,r}^\sigma(r') J_{n+1}(q_2 r') r' dr', \tag{E8}$$

$$Q_{n>}^\sigma(r) = \frac{1}{\tau_2^\sigma}\int_r^a p_{n+,r}^\sigma(r') H_{n+1}^{(1)}(q_2 r') r' dr'. \tag{E9}$$

The amplitudes $\tilde{H}_{2rn}^\phi$, $\tilde{H}_{2\theta n}^\phi$, and $\tilde{H}_{2zn}^\phi$ can be formally obtained from $\tilde{E}_{2rn}^\phi$, $\tilde{E}_{2\theta n}^\phi$, and $\tilde{E}_{2zn}^\phi$, respectively, using the substitutions

$$\begin{aligned} P_{n\nu}^e &\to P_{n\nu}^m, \quad Q_{n\nu}^e \to Q_{n\nu}^m,\\ P_{n\nu}^m &\to -\epsilon_2 P_{n\nu}^e, \quad Q_{n\nu}^m \to -\epsilon_2 Q_{n\nu}^e,\\ \tau_2^e &\to \tau_2^m, \quad p_{n\pm,r}^e \to p_{n\pm,r}^m,\end{aligned} \tag{E10}$$

where the subscript $\nu$ acquires the values $<$ or $>$. Let us note that

$$P_{n>}^\sigma(a) = Q_{n>}^\sigma(a) = 0. \tag{E11}$$

## APPENDIX F: EXPLICIT FORM OF THE MATRICES $\hat{M}_n$ AND $\hat{N}_n$

The matrix $\hat{M}_n$ has the following form:

$$\hat{M}_n(\beta) = \begin{pmatrix} \left(\beta n/q_2^2 a\right)J_n(q_2 a) & -(i\omega/cq_2)J_n'(q_2 a) & -\left(\beta n/q_1^2 a\right)H_n^{(1)}(q_1 a) & (i\omega/cq_1)H_n^{(1)\prime}(q_1 a)\\ J_n(q_2 a) & 0 & -H_n^{(1)}(q_1 a) & 0\\ \left(ik_2^2 c/\omega q_2\right)J_n'(q_2 a) & \left(\beta n/q_2^2 a\right)J_n(q_2 a) & -\left(ik_1^2 c/\omega q_1\right)H_n^{(1)\prime}(q_1 a) & -\left(\beta n/q_1^2 a\right)H_n^{(1)}(q_1 a)\\ 0 & J_n(q_2 a) & 0 & -H_n^{(1)}(q_1 a)\end{pmatrix}, \tag{F1}$$

where the prime above the Bessel and Hankel functions denotes their derivative with respect to their argument.

The matrix elements of the matrix $\hat{N}_n$ are found as follows:

$$[\hat{N}_n(\beta,\beta')]_{11} = \frac{\pi^2}{\omega}\Big\{ -\Big[ik_2^2\pi^{e,1}_{2,-1}(\beta,\beta') + \frac{\omega}{c}\beta\pi^{m,1}_{2,-1}(\beta,\beta')\Big]H^{(1)}_{n-1}(q_2a) + \Big[ik_2^2\pi^{e,1}_{2,1}(\beta,\beta') - \frac{\omega}{c}\beta\pi^{m,1}_{2,1}(\beta,\beta')\Big]H^{(1)}_{n+1}(q_2a) + i\frac{nq_2}{a}\big[\pi^{e,1}_{2,-1}(\beta,\beta') - \pi^{e,1}_{2,1}(\beta,\beta')\big]H^{(1)}_n(q_2a)\Big\}, \tag{F2}$$

$$[\hat{N}_n(\beta,\beta')]_{12} = \frac{\pi^2}{\omega}\Big\{ -\Big[ik_2^2\pi^{e,2}_{2,-1}(\beta,\beta') + \frac{\omega}{c}\beta\pi^{m,2}_{2,-1}(\beta,\beta')\Big]H^{(1)}_{n-1}(q_2a) + \Big[ik_2^2\pi^{e,2}_{2,1}(\beta,\beta') - \frac{\omega}{c}\beta\pi^{m,2}_{2,1}(\beta,\beta')\Big]H^{(1)}_{n+1}(q_2a) + i\frac{nq_2}{a}\big[\pi^{e,2}_{2,-1}(\beta,\beta') - \pi^{e,2}_{2,1}(\beta,\beta')\big]H^{(1)}_n(q_2a)\Big\}, \tag{F3}$$

$$[\hat{N}_n(\beta,\beta')]_{13} = \frac{\pi^2}{\omega}\Big\{\Big[ik_1^2\pi^{e,3}_{1,-1}(\beta,\beta') + \frac{\omega}{c}\beta\pi^{m,3}_{1,-1}(\beta,\beta')\Big]J_{n-1}(q_1a) - \Big[ik_1^2\pi^{e,3}_{1,1}(\beta,\beta') - \frac{\omega}{c}\beta\pi^{m,3}_{1,1}(\beta,\beta')\Big]J_{n+1}(q_1a) - i\frac{nq_1}{a}\big[\pi^{e,3}_{1,-1}(\beta,\beta') - \pi^{e,3}_{1,1}(\beta,\beta')\big]J_n(q_1a)\Big\}, \tag{F4}$$

$$[\hat{N}_n(\beta,\beta')]_{14} = \frac{\pi^2}{\omega}\Big\{\Big[ik_1^2\pi^{e,4}_{1,-1}(\beta,\beta') + \frac{\omega}{c}\beta\pi^{m,4}_{1,-1}(\beta,\beta')\Big]J_{n-1}(q_1a) - \Big[ik_1^2\pi^{e,4}_{1,1}(\beta,\beta') - \frac{\omega}{c}\beta\pi^{m,4}_{1,1}(\beta,\beta')\Big]J_{n+1}(q_1a) - i\frac{nq_1}{a}\big[\pi^{e,4}_{1,-1}(\beta,\beta') - \pi^{e,4}_{1,1}(\beta,\beta')\big]J_n(q_1a)\Big\}, \tag{F5}$$

$$[\hat{N}_n(\beta,\beta')]_{21} = -\frac{\pi^2}{\omega}q_2\Big\{i\beta\big[\pi^{e,1}_{2,-1}(\beta,\beta') - \pi^{e,1}_{2,1}(\beta,\beta')\big] + \frac{\omega}{c}\big[\pi^{m,1}_{2,-1}(\beta,\beta') + \pi^{m,1}_{2,1}(\beta,\beta')\big]\Big\}H^{(1)}_n(q_2a), \tag{F6}$$

$$[\hat{N}_n(\beta,\beta')]_{22} = -\frac{\pi^2}{\omega}q_2\Big\{i\beta\big[\pi^{e,2}_{2,-1}(\beta,\beta') - \pi^{e,2}_{2,1}(\beta,\beta')\big] + \frac{\omega}{c}\big[\pi^{m,2}_{2,-1}(\beta,\beta') + \pi^{m,2}_{2,1}(\beta,\beta')\big]\Big\}H^{(1)}_n(q_2a), \tag{F7}$$

$$[\hat{N}_n(\beta,\beta')]_{23} = \frac{\pi^2}{\omega}q_1\Big\{i\beta\big[\pi^{e,3}_{1,-1}(\beta,\beta') - \pi^{e,3}_{1,1}(\beta,\beta')\big] + \frac{\omega}{c}\big[\pi^{m,3}_{1,-1}(\beta,\beta') + \pi^{m,3}_{1,1}(\beta,\beta')\big]\Big\}J_n(q_1a), \tag{F8}$$

$$[\hat{N}_n(\beta,\beta')]_{24} = \frac{\pi^2}{\omega}q_1\Big\{i\beta\big[\pi^{e,4}_{1,-1}(\beta,\beta') - \pi^{e,4}_{1,1}(\beta,\beta')\big] + \frac{\omega}{c}\big[\pi^{m,4}_{1,-1}(\beta,\beta') + \pi^{m,4}_{1,1}(\beta,\beta')\big]\Big\}J_n(q_1a), \tag{F9}$$

$$[\hat{N}_n(\beta,\beta')]_{31} = \frac{\pi^2}{\omega}\Big\{ -\Big[ik_2^2\pi^{m,1}_{2,-1}(\beta,\beta') - \frac{\omega}{c}\beta\epsilon_2\pi^{e,1}_{2,-1}(\beta,\beta')\Big]H^{(1)}_{n-1}(q_2a) + \Big[ik_2^2\pi^{m,1}_{2,1}(\beta,\beta') + \frac{\omega}{c}\beta\epsilon_2\pi^{e,1}_{2,1}(\beta,\beta')\Big]H^{(1)}_{n+1}(q_2a) + i\frac{nq_2}{a}\big[\pi^{m,1}_{2,-1}(\beta,\beta') - \pi^{m,1}_{2,1}(\beta,\beta')\big]H^{(1)}_n(q_2a)\Big\}, \tag{F10}$$

$$[\hat{N}_n(\beta,\beta')]_{32} = \frac{\pi^2}{\omega}\Big\{ -\Big[ik_2^2\pi^{m,2}_{2,-1}(\beta,\beta') - \frac{\omega}{c}\beta\epsilon_2\pi^{e,2}_{2,-1}(\beta,\beta')\Big]H^{(1)}_{n-1}(q_2a) + \Big[ik_2^2\pi^{m,2}_{2,1}(\beta,\beta') + \frac{\omega}{c}\beta\epsilon_2\pi^{e,2}_{2,1}(\beta,\beta')\Big]H^{(1)}_{n+1}(q_2a) + i\frac{nq_2}{a}\big[\pi^{m,2}_{2,-1}(\beta,\beta') - \pi^{m,2}_{2,1}(\beta,\beta')\big]H^{(1)}_n(q_2a)\Big\}, \tag{F11}$$

$$[\hat{N}_n(\beta,\beta')]_{33} = \frac{\pi^2}{\omega}\Big\{\Big[ik_1^2\pi^{m,3}_{1,-1}(\beta,\beta') - \frac{\omega}{c}\beta\epsilon_1\pi^{e,3}_{1,-1}(\beta,\beta')\Big]J_{n-1}(q_1a) - \Big[ik_1^2\pi^{m,3}_{1,1}(\beta,\beta') + \frac{\omega}{c}\beta\epsilon_1\pi^{e,3}_{1,1}(\beta,\beta')\Big]J_{n+1}(q_1a) - i\frac{nq_1}{a}\big[\pi^{m,3}_{1,-1}(\beta,\beta') - \pi^{m,3}_{1,1}(\beta,\beta')\big]J_n(q_1a)\Big\}, \tag{F12}$$

$$[\hat{N}_n(\beta,\beta')]_{34} = \frac{\pi^2}{\omega}\Big\{\Big[ik_1^2\pi^{m,4}_{1,-1}(\beta,\beta') - \frac{\omega}{c}\beta\epsilon_1\pi^{e,4}_{1,-1}(\beta,\beta')\Big]J_{n-1}(q_1a) - \Big[ik_1^2\pi^{m,4}_{1,1}(\beta,\beta') + \frac{\omega}{c}\beta\epsilon_1\pi^{e,4}_{1,1}(\beta,\beta')\Big]J_{n+1}(q_1a) - i\frac{nq_1}{a}\big[\pi^{m,4}_{1,-1}(\beta,\beta') - \pi^{m,4}_{1,1}(\beta,\beta')\big]J_n(q_1a)\Big\}, \tag{F13}$$

$$[\hat{N}_n(\beta,\beta')]_{41} = -\frac{\pi^2}{\omega}q_2\Big\{i\beta\big[\pi^{m,1}_{2,-1}(\beta,\beta') - \pi^{m,1}_{2,1}(\beta,\beta')\big] - \frac{\omega}{c}\epsilon_2\big[\pi^{e,1}_{2,-1}(\beta,\beta') + \pi^{e,1}_{2,1}(\beta,\beta')\big]\Big\}H^{(1)}_n(q_2a), \tag{F14}$$

$$[\hat{N}_n(\beta,\beta')]_{42} = -\frac{\pi^2}{\omega} q_2 \left\{ i\beta \left[ \pi^{m,2}_{2,-1}(\beta,\beta') - \pi^{m,2}_{2,1}(\beta,\beta') \right] - \frac{\omega}{c} \epsilon_2 \left[ \pi^{e,2}_{2,-1}(\beta,\beta') + \pi^{e,2}_{2,1}(\beta,\beta') \right] \right\} H^{(1)}_n(q_2 a), \tag{F15}$$

$$[\hat{N}_n(\beta,\beta')]_{43} = \frac{\pi^2}{\omega} q_1 \left\{ i\beta \left[ \pi^{m,3}_{1,-1}(\beta,\beta') - \pi^{m,3}_{1,1}(\beta,\beta') \right] - \frac{\omega}{c} \epsilon_1 \left[ \pi^{e,3}_{1,-1}(\beta,\beta') + \pi^{e,3}_{1,1}(\beta,\beta') \right] \right\} J_n(q_1 a), \tag{F16}$$

$$[\hat{N}_n(\beta,\beta')]_{44} = \frac{\pi^2}{\omega} q_1 \left\{ i\beta \left[ \pi^{m,4}_{1,-1}(\beta,\beta') - \pi^{m,4}_{1,1}(\beta,\beta') \right] - \frac{\omega}{c} \epsilon_1 \left[ \pi^{e,4}_{1,-1}(\beta,\beta') + \pi^{e,4}_{1,1}(\beta,\beta') \right] \right\} J_n(q_1 a). \tag{F17}$$

Here we have introduced the following functions:

$$\pi^{\sigma,k}_{j,\mu}(\beta,\beta') = \frac{1}{\tau^\sigma_j} \frac{a}{\beta^2 - \beta'^2} C^{\sigma,k}_{j,\mu}(\beta') D_{j,\mu}(\beta,\beta'), \tag{F18}$$

where $\sigma = e,m$; $k = 1,2,3,4$; $j = 1,2$; $\mu = \pm 1$; $\tau^e_j = \epsilon_j$; $\tau^m_j = 1$; and

$$C^{e,1}_{2,1}(\beta) = -C^{e,1}_{2,-1}(\beta) = i \frac{c^2 k_2^2}{4\pi\omega q_2}; \tag{F19}$$

$$C^{e,2}_{2,1}(\beta) = C^{e,2}_{2,-1}(\beta) = -\frac{c\beta}{4\pi q_2}; \tag{F20}$$

$$C^{e,3}_{1,1}(\beta) = -C^{e,3}_{1,-1}(\beta) = -i \frac{c^2 k_1^2}{4\pi\omega q_1}; \tag{F21}$$

$$C^{e,4}_{1,1}(\beta) = C^{e,4}_{1,-1}(\beta) = \frac{c\beta}{4\pi q_1}; \tag{F22}$$

$$C^{m,1}_{2,1}(\beta) = C^{m,1}_{2,-1}(\beta) = \frac{c\beta}{4\pi q_2}; \tag{F23}$$

$$C^{m,2}_{2,1}(\beta) = -C^{m,2}_{2,-1}(\beta) = i \frac{\omega}{4\pi q_2}; \tag{F24}$$

$$C^{m,3}_{1,1}(\beta) = C^{m,3}_{1,-1}(\beta) = -\frac{c\beta}{4\pi q_1}; \tag{F25}$$

$$C^{m,4}_{1,1}(\beta) = -C^{m,4}_{1,-1}(\beta) = -i \frac{\omega}{4\pi q_1}; \tag{F26}$$

$$D_{j,\mu}(\beta,\beta') = q'_j Z_{n+\mu}(q_j a) Z_{n+\mu-1}(q'_j a) - q_j Z_{n+\mu-1}(q_j a) Z_{n+\mu}(q'_j a); \tag{F27}$$

with $q'_j = \sqrt{k_j^2 - \beta'^2}$ and

$$Z_m(q_j a) = \begin{cases} H^{(1)}_m(q_1 a) & \text{if } j = 1, \\ J_m(q_2 a) & \text{if } j = 2. \end{cases} \tag{F28}$$

When calculating the matrix elements of $\hat{N}_n(\beta,\beta')$ at $\beta' \to \beta$ one should use the limit

$$\lim_{\beta' \to \beta} \pi^{\sigma,k}_{j,\mu}(\beta,\beta') = -\frac{a^2}{2\tau^\sigma_j} C^{\sigma,k}_{j,\mu}(\beta) D^0_{j,\mu}(\beta) \tag{F29}$$

with

$$D^0_{j,\mu}(\beta) = [Z_{n+\mu}(q_j a)]^2 - Z_{n+\mu-1}(q_j a) Z_{n+\mu+1}(q_j a). \tag{F30}$$

## APPENDIX G: EXPLICIT FORM OF THE FUNCTIONS $\lambda^\sigma_{jvn}(r)$ AND $\mu^\sigma_{vn}(r)$

The functions $\lambda^\sigma_{jvn}(r)$ and $\mu^\sigma_{vn}(r)$ with $v = r,\theta$ which determine the quantities $\mathbf{q}^\sigma_{jn\pm}(r)$ are found as follows:

$$\lambda^e_{jrn}(r) = -\frac{c}{8\pi^2} \int_C \tilde{H}^\psi_{j\theta n}(r;\beta) e^{i\beta L/2} d\beta, \tag{G1}$$

$$\lambda^e_{j\theta n}(r) = \frac{c}{8\pi^2} \int_C \tilde{H}^\psi_{jrn}(r;\beta) e^{i\beta L/2} d\beta, \tag{G2}$$

$$\lambda^m_{jrn}(r) = \frac{c}{8\pi^2} \int_C \tilde{E}^\psi_{j\theta n}(r;\beta) e^{i\beta L/2} d\beta, \tag{G3}$$

$$\lambda^m_{j\theta n}(r) = -\frac{c}{8\pi^2} \int_C \tilde{E}^\psi_{jrn}(r;\beta) e^{i\beta L/2} d\beta, \tag{G4}$$

$$\mu^e_{rn}(r) = -\frac{c}{8\pi^2} \int_C \tilde{H}^\phi_{2\theta n}(r;\beta) e^{i\beta L} d\beta, \tag{G5}$$

$$\mu^e_{\theta n}(r) = \frac{c}{8\pi^2} \int_C \tilde{H}^\phi_{2rn}(r;\beta) e^{i\beta L} d\beta, \tag{G6}$$

$$\mu^m_{rn}(r) = \frac{c}{8\pi^2} \int_C \tilde{E}^\phi_{2\theta n}(r;\beta) e^{i\beta L} d\beta, \tag{G7}$$

$$\mu^m_{\theta n}(r) = -\frac{c}{8\pi^2} \int_C \tilde{E}^\phi_{2rn}(r;\beta) e^{i\beta L} d\beta, \tag{G8}$$

where the Fourier-transformed field amplitudes $\tilde{E}^{\psi,\phi}_{jvn}$ and $\tilde{H}^{\psi,\phi}_{jvn}$ are given in Appendices E and C.

*bordo@mci.sdu.dk; Former address: A. M. Prokhorov General Physics Institute, Russian Academy of Sciences, 119991 Moscow, Russia.

[1] F. J. Garcia-Vidal, L. Martin-Moreno, T. W. Ebbesen, and L. Kuipers, Rev. Mod. Phys. **82**, 729 (2010).

[2] T. W. Ebbesen, H. J. Lezec, H. F. Ghaemi, T. Thio, and P. A. Wolff, Nature (London) **391**, 667 (1998).

[3] A. Degiron, H. J. Lezec, N. Yamamoto, and T. W. Ebbesen, Opt. Commun. **239**, 61 (2004).

[4] J. Prikulis, P. Hanarp, L. Olofsson, D. Sutherland, and M. Käll, Nano Lett. **4**, 1003 (2004).

[5] R. Wannemacher, Opt. Commun. **195**, 107 (2001).

[6] E. Popov, N. Bonod, M. Nevière, H. Rigneault, P.-F. Lenne, and P. Chaumet, Appl. Opt. **44**, 2332 (2005).

[7] S.-H. Chang, S. K. Gray, and G. C. Schatz, Opt. Express **13**, 3150 (2005).

[8] E. Eremina, Y. Eremin, N. Grishina, and T. Wriedt, J. Comput. Theor. Nanosci. **6**, 795 (2009).

[9]F. J. García de Abajo, Opt. Express **10**, 1475 (2002).
[10]C.-W. Chang, A. K. Sarychev, and V. M. Shalaev, Laser Phys. Lett. **2**, 351 (2005).
[11]F. J. García-Vidal, E. Moreno, J. A. Porto, and L. Martín-Moreno, Phys. Rev. Lett. **95**, 103901 (2005).
[12]A. Yu. Nikitin, D. Zueco, F. J. García-Vidal, and L. Martín-Moreno, Phys. Rev. B **78**, 165429 (2008).
[13]H. J. Lezec and T. Thio, Opt. Express **12**, 3629 (2004).
[14]H. A. Bethe, Phys. Rev. **66**, 163 (1944).
[15]C. J. Bouwkamp, Philips Res. Rep. **5**, 321 (1950).
[16]Let us note that the analytical expressions for the diffracted field in this case were obtained in a different form in the paper by V. V. Klimov and V. S. Letokhov, Opt. Commun. **106**, 151 (1994). The author thanks V. V. Petrunin, who brought this reference to his knowledge.
[17]A. Roberts, J. Opt. Soc. Am. A **4**, 1970 (1987).
[18]G. Colas des Francs, D. Molenda, U. C. Fischer, and A. Naber, Phys. Rev. B **72**, 165111 (2005).
[19]B. Sepúlveda, Y. Alaverdyan, J. Alegret, M. Käll, and P. Johansson, Opt. Express **16**, 5609 (2008).
[20]V. G. Bordo, Phys. Rev. B **81**, 035420 (2010).
[21]J. A. Stratton, *Electromagnetic Theory* (McGraw-Hill, New York, 1941).
[22]M. Born and E. Wolf, *Principles of Optics: Electromagnetic Theory of Propagation, Interference and Diffraction of Light* (Cambridge University Press, Cambridge, 1997).
[23]S. A. Schelkunoff, Phys. Rev. **56**, 308 (1939).
[24]I. S. Gradshteyn and I. M. Ryzhik, *Table of Integrals, Series and Products* (Academic Press, New York, 1994).
[25]P. B. Johnson and R. W. Christy, Phys. Rev. B **6**, 4370 (1972).
[26]A. Sommerfeld, *Partial Differential Equations in Physics*, Lectures on Theoretical Physics, Vol. VI (Academic Press, New York, London, 1964).
[27]L. Yin, V. K. Vlasko-Vlasov, A. Rydh, J. Pearson, U. Welp, S.-H. Chang, S. K. Gray, G. C. Schatz, D. B. Brown, and C. W. Kimball, Appl. Phys. Lett. **85**, 467 (2004).
[28]A defective structure of the hole rim can be seen, for example, in the SEM image of a subwavelength hole presented in Ref. 3.
[29]A. Yu. Nikitin, F. J. García-Vidal, and L. Martín-Moreno, Phys. Rev. Lett. **105**, 073902 (2010).